R. E. Mach
T. L. Gardner

Rectification of Satellite Photography by Digital Techniques*

Abstract: Sample photographs from the TIROS I Weather Satellite have been successfully transformed into a Mercator projection using automatic digital techniques. Mathematical formulas expressing the relation between the photoplane and the Mercator projection have been derived, and a computer program has been written to efficiently manipulate a "digital photograph" in accordance with the formulas.

Introduction

TIROS I was an experimental weather observation satellite equipped to transmit visual images of cloud cover back to earth. The 23,000 pictures received from TIROS I testified to its success. These pictures contained much significant meteorological information, but use of manual methods to determine the location of each image and to rectify it, i.e., determine its scale and orientation, posed a problem. Manual methods for TIROS I involve the preparation of grid networks drawn to the same scale and perspective as the visual images obtained from the satellite. These grids are used in conjunction with horizon curves and computer-predicted location data to determine the orientation of the images. After fitting the appropriate grid to each picture, manual techniques are employed to transfer the key data from the perspective photo view to an oblique Mercator grid. The process requires skilled analysts to select the significant features, which are then carefully plotted using various symbols to represent cloud features.

Coming generations of weather satellites will transmit three times as many pictures per orbit than present TIROS satellites. Clearly, if this deluge of satellite weather data is to be fully utilized, means of organizing the data automatically must be developed.

At the time of the initial TIROS satellite launchings, the IBM Federal Systems Division Command Control Center at Kingston, N.Y., was experimenting with the automatic digital processing of stereo pairs of aerial photographs to produce orthophotographs with elevation contours. Because of the large number of usable TIROS photographs which were being received and the largely manual methods being employed in their processing, plans were made to automate the rectification process using digital image processing techniques.

By using a digital computer, it is possible to reconstruct the contents of the entire image in Mercator projection. In addition, the flexibility of the technique permits adaptation of the process to other projections, if desired. Important cloud features might also be automatically extracted to facilitate analysis and data transmission.

The basic scheme is to determine the gray tone of discrete picture elements and establish the relative location of each element in the original image. A cathode-ray tube scanning device is employed to obtain this representation of the image, and the data is then recorded in digital form on magnetic tape in the order in which it was scanned. A digital computer, programmed to rearrange the data according to the mathematical formulations which describe the relation between the old and new formats, generates the new image.

The digital output image is placed on magnetic tape, which is then played back using the scanning equipment in the reverse mode to create the new image on film. A unique feature of this technique is that the digitizing and reproduction operations are performed off-line, i.e., the computer is not involved in these operations.

* The research reported in this paper has been sponsored by the Geophysics Research Directorate of the Air Force, Cambridge Research Laboratories, Office of Aerospace Research under Contract AF 19(604) 8432.

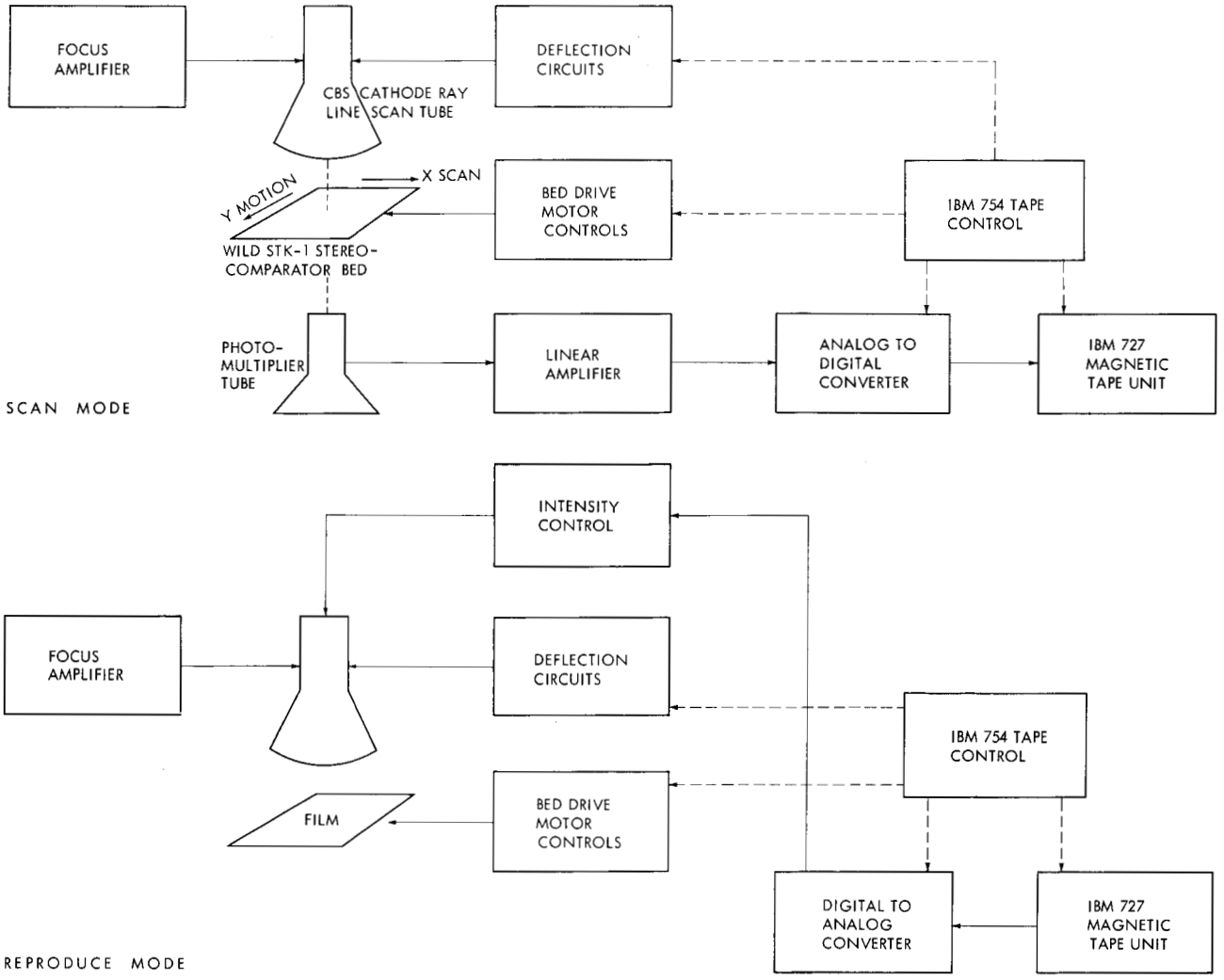

Figure 1 **Digitizing system diagram.**

The rectification process

• *Generation of digital data*

Digital data is produced from photographic film using the system shown in Fig. 1. The first step in the conversion process is the generation of an electric analog of the gray tones of the image. This is accomplished using a cathode-ray tube as a flying-spot light source which is successively focused on discrete areas of the film. The light transmitted by the film energizes a photomultiplier tube to produce an electric current which is proportional to the transmissivity of the film.

The photomultiplier signal is passed through an amplifier to an analog-to-digital converter. The converter reduces the voltage to one of eight digital values, 0 for black through 7 for white.

The digital output, in binary form, requires three bits to represent the eight gray values. The digital data from the converter is recorded on magnetic tape as individual tape characters using an IBM 727 magnetic tape unit. The entire operation is controlled by the oscillator in an associated IBM 754 tape control unit. With the image represented in digital form on magnetic tape, it can be processed in the digital computer.

The cathode-ray tube and photomultiplier are installed on a modified WILD STK-1 stereocomparator shown in Fig. 2.* Scanning is accomplished using the CRT sweep in the x coordinate; the entire film is scanned by successive movements of the comparator bed in the y coordinate. The character rate of the IBM 727 tape unit (15,000 characters per second) determines the operating speed of the system. A TIROS 35 mm picture can be scanned in approximately two minutes. The scanning time depends on the size of the included border area around the actual

* The modification of the stereocomparator was accomplished under U.S. Army GIMRADA Contract 44-009 ENG 4724, for Fort Belvoir, Va.

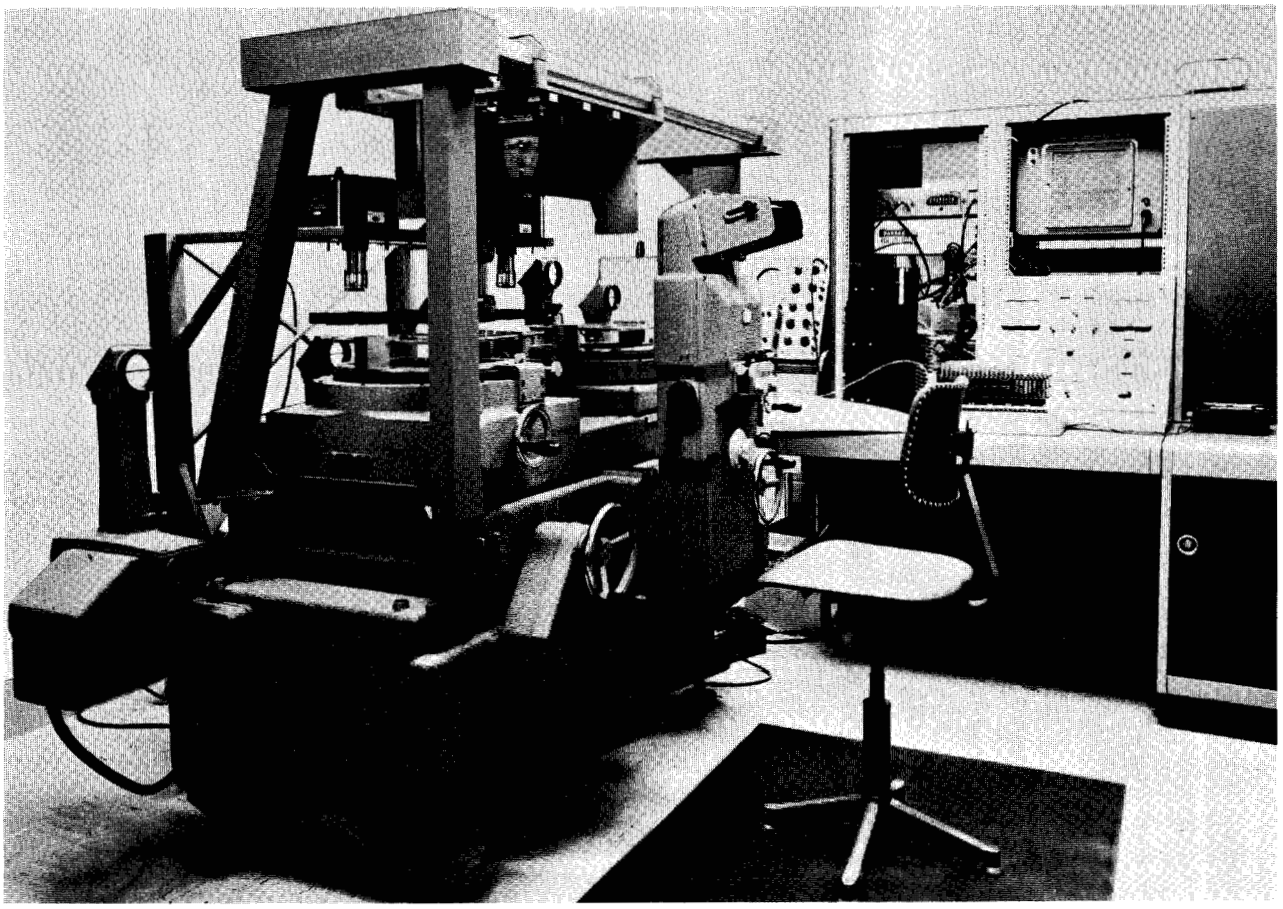

Figure 2 **Modified WILD STK-1 stereocomparator.**

image. Because the scanning equipment is designed to process $4\frac{1}{2}$-inch photographs, a corresponding sweep is generated but the excess blank "data" is not recorded. Scanning and digitizing in a system designed specifically for 35 mm images would take about 10 seconds, using the same tape rate of 15 kc. A scan resolution of 16 lines/mm (406 lines/in) was used for the TIROS images. This density reduced the 0.75 × 0.75 in. image to 90,000 characters of digital data.

Difficulty encountered in digitizing certain sample photographs was due to the response of the scanning equipment to changes in image density. The voltage output V_0 from the photomultipliers is a linear function of the light intensity I_2, impinging on the photomultiplier cathode, $V_0 = KI_2$. The intensity reaching the cathode $I_2 = I_1 \times T$, where I_1 is the intensity of the light source after passing through the optical system and T is the transmissivity of the film. Because a linear amplifier of gain A was used to provide the voltage required for the A/D converter, the voltage which was digitized V_d was directly proportional to the transmissivity of the film image at the spot being scanned, $V_d = AV_0 = AKI_1T$. However, the human eye is essentially a logarithmic sensor, and rather than express the light transmission characteristics of film in terms of transmissivity, the parameter density $D = \log 1/T$ is used. The eye responds directly to density changes in a photographic image. A good quality photograph has a density range from 0.0 to something greater than 2.0. This represents a change from 1.0 to 0.01 or less in the film transmissivity between the lightest and darkest areas of the film. With the scanning system responding directly to transmissivity as described previously, the largest density range that could be discerned was about 0.5. TIROS orbit 638, consisting of low-contrast images, contained densities from 0.35 to 0.80. Thus, the 0.5 density range covered these extremes and gray shade rendering was obtained. However, two other orbits, 016 and 703, had density extremes of 0.0 and 1.70, and the results were poor. The obvious solution to this problem is to replace the linear amplifier with one having a logarithmic response curve. Unfortunately, this was not available at the time the pictures were being processed. An alternative method was used which consisted of reducing the contrast of the images photographically prior to processing. Although the information content of the image was reduced, con-

trast reduction was considered acceptable because the primary objective was to demonstrate digital automatic rectification. Gray tone fidelity was considered secondary at this stage of development.

Digital processing of data

• *Overall concept*

To perform digital image processing, the relation between the original and the desired new format must be expressible mathematically. In addition to the mathematical formulation, the orientation of the image plane relative to the earth must be established. The orientation is described by seven parameters:* latitude and longitude of the sub-satellite point; latitude and longitude of the image principal point; altitude of the satellite; nadir angle of the picture; and swing or azimuth angle of the image about the principal axis. These data were supplied by the Geophysics Research Directorate for each frame and placed on punch cards for the computer program.

With the mathematical expression and controlling parameters defined, data points in the original format are transformed, as required, into their new format. The desired format for TIROS images was selected as a Mercator projection with tangency at the equator. Two reasons support this selection. First, the Mercator projection is familiar to meteorologists who would be most interested in the transformed image data. Second, the Mercator projection, with the lines of latitude and longitude forming a rectangular grid, lends itself to the mosaic formation of large areas from overlapping images. The selection of the Mercator projection does not obviate other projections. For polar orbit weather satellites, a polar stereographic projection would be most practical. Obviously, the Mercator projection which is satisfactory in the regions covered by TIROS I would be inadequate in the polar regions. The governing criterion is the availability of a mathematical expression for the desired projection system.

The first step required for any satellite mapping procedure is the transformation of points in the image plane to their true locations on the earth's surface. This is accomplished in two phases. First, the image plane is projected to the surface of an arbitrary sphere, Fig. 3, whose polar axis coincides with the nadir axis of the photograph. With the points established in their relative position on this sphere, the second phase involves obtaining their true location on the earth's surface via three coordinate rotations. The mathematical formulas are developed in Appendix 1.

With the points located in true earth coordinates, previously derived mathematical expressions are used to obtain the Mercator projection of the data.

After establishing the image-to-Mercator-projection transformation, a program had to be generated which would produce the corrected image by manipulating the discrete points of the image represented by the digital data with the least possible computation time.

• *Program philosophy*

To minimize the time required to process a TIROS photograph on the computer, a general flow of the necessary steps was developed. It became apparent that the actual point coordinate transformation was the greatest single time-consuming element. Elimination of redundant points was studied as a means of reducing the amount of data. Considerable redundant data is present in photographs which have areas of constant gray values. Actually, only coordinates of the outline or border of the areas and their shade values need be considered, if we somehow note that no change occurs in the interior.

This technique, demonstrated in Fig. 4, was applied by searching through the input data on a line-by-line basis for points where the gray-shade values changed. The rectilinear grid on the original image in Fig. 4 represents the coordinates of the digitized data. The free-form represents a cloud and the heavy line is a portion of a scan line with constant gray value. The gray value changes at each end of the line. In the Mercator projection, the original rectilinear grid has been transformed to the curvilinear grid. The rectilinear grid here is the x-y coordinate system in the computer memory in which the output image is formed. The heavy line represents the mapped image of the original segment. The only points mapped in the output image were those whose shade value changed. The intermediate points of constant shade value along an output line segment were filled by linear interpolation. Thus, a reduction in the number of data points was achieved. The amount of reduction varied with the length of the line segment, i.e., the amount of detail present in the image.

Certain complications attended the use of this technique. Because the mapping process takes place via a spherical surface, rectangular grids in the input or image plane do not retain their rectangular nature in the Mercator projection as shown in Fig. 5. The input image in this case was a checkerboard test pattern consisting of squares with 18 data points on each side. The checkerboard was used because this form of data is also a severe test for the program. By applying certain tilt and swing parameters to the data, the Mercator projection was obtained as shown. The degree of curvature introduced depends on the magnitude of the nadir angle, the latitude of the area on the image, and the proximity of the area to the horizon in the image. It can be seen that we are not free to use linear interpolation without prudence. If the distance between the points where the gray shade value changes exceeds certain limits, which depend on the above-mentioned factors, the space between the two points on the Mercator projection will be occupied by a curved rather than a straight line. In addition, lines of

* The seven parameters indicated above could be reduced to six if, instead of the coordinates of the principal point, the azimuth angle of the principal point from the sub-satellite point is used.

data which were adjacent in the input data can spread apart, as is evidenced by the stretching which has taken place in the lower left-hand corner of the checkerboard image.

The following rules were established to account for these complications. It was noted that the curve could be represented by a straight line in the Mercator projection if its deviation from a straight line did not exceed one-half of the scanning resolution. Further study confirmed that a distance between input data points of 16 spaces would meet this resolution criterion for most cases. Only near the horizon was it necessary to reduce the distance to six spaces. If the line length between shade changes exceeded these

Figure 3 **Relationship between image plane and earth sphere.**

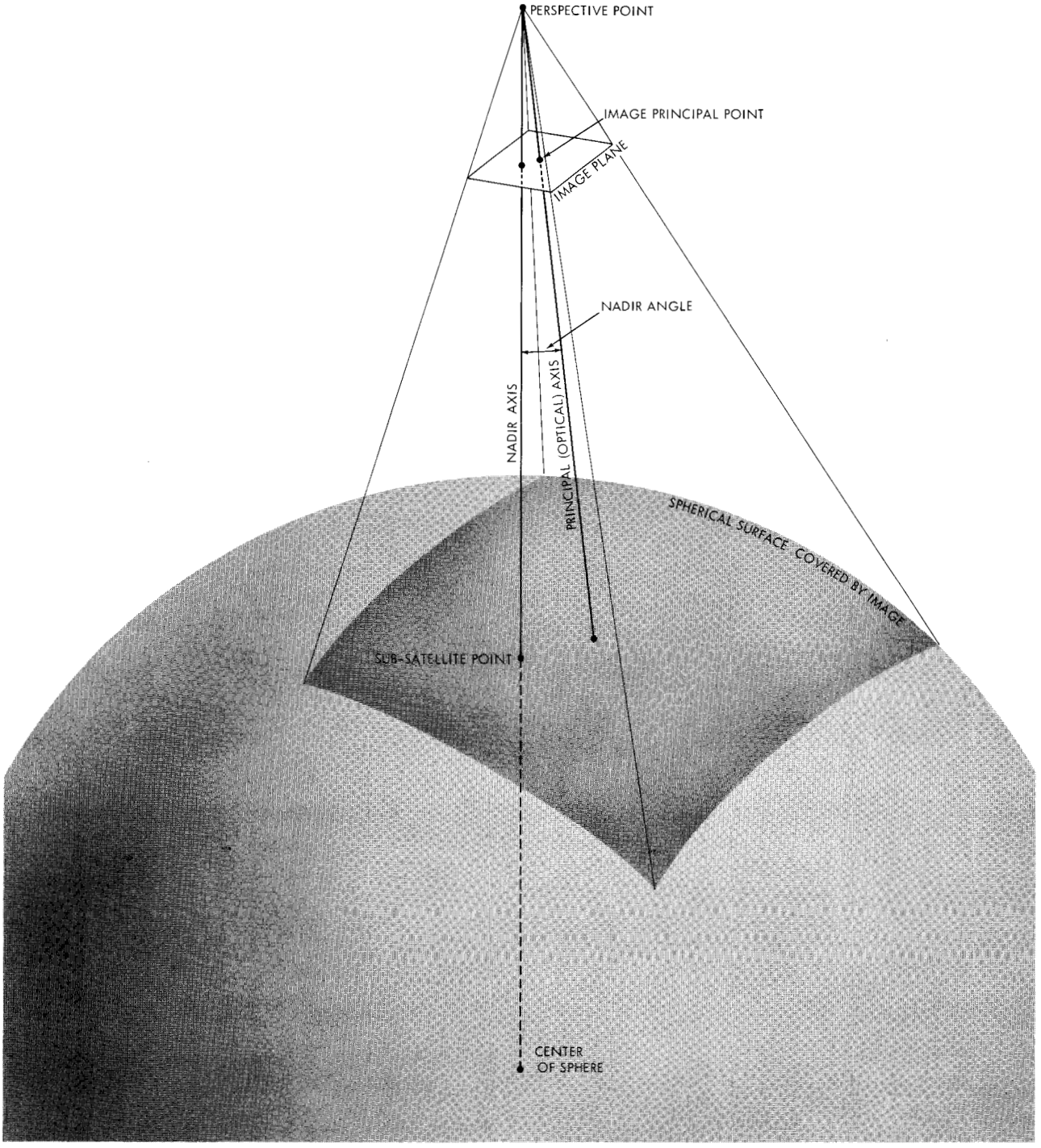

criteria, additional points were mapped as required. The expansion situation was handled by a filling-in process which was performed after all the original data points had been mapped, either directly or due to linear interpolations along the line segments between points.

Utilizing these techniques, the program stored the image data from magnetic tape in core memory together with the contents of a data card containing the orientation parameters of the image. Basic constants used in the process were computed and the matrices which describe the mapping process were established. Then data points were mapped, line segment by line segment, until all points in the original

Figure 4 **Mapping of line segment.**
Left: Original perspective image. Right: Mercator projection image.

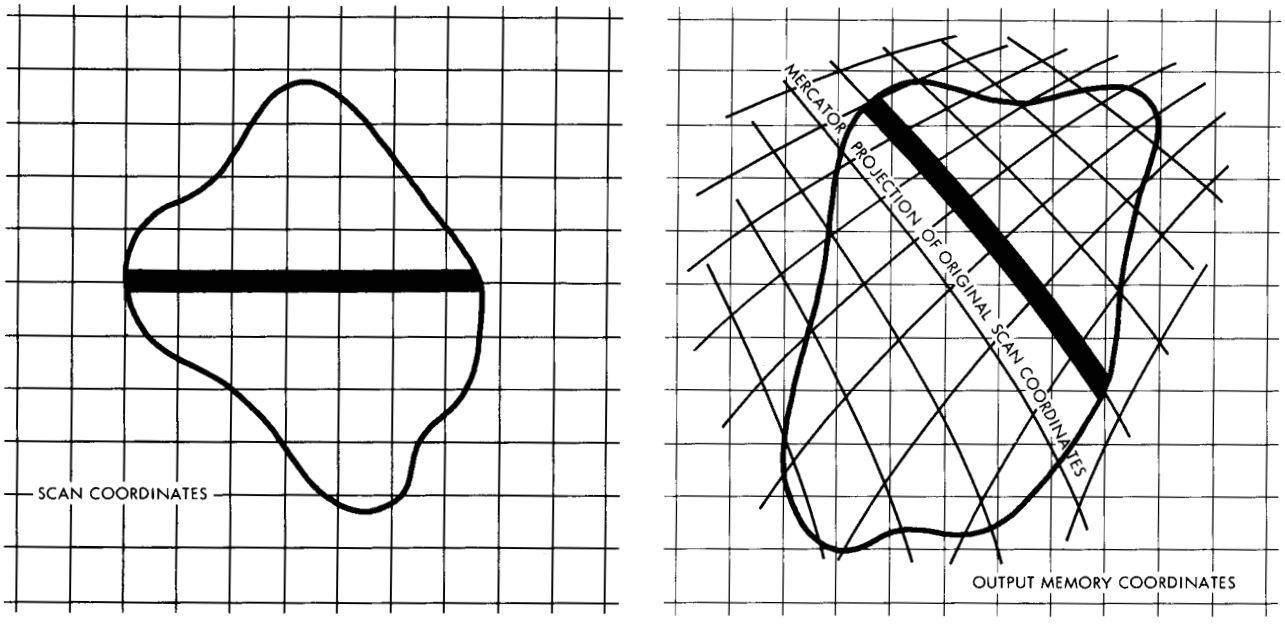

Figure 5 **Checkerboard test pattern.**
Left: Input image. Right: Mercator projection image.

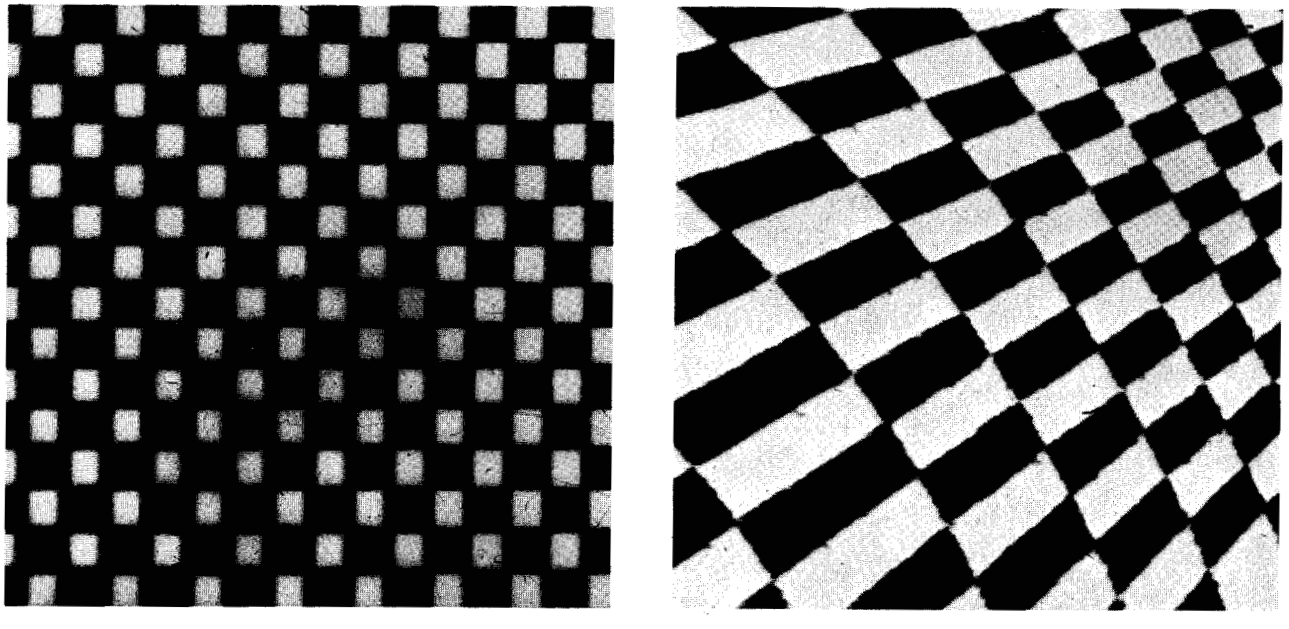

image were processed. Any unfilled locations in the rectified image caused by expansion were then filled in and the completed image stored on magnetic tape. A simultaneous printed output contained the frame number and the earth coordinates in latitude and longitude of the center of the rectified image.

• *Distortions*

In addition to obtaining a Mercator projection of the photographic image of the earth's cloud cover, other changes or corrections to the data may be accomplished if they can be expressed mathematically. Examples include corrections for atmospheric and optical distortion, which affect the geometry of the image.

During this phase of the project, the effects of atmospheric distortion were examined.

The refraction of light rays which focus at the perspective point of the photo image varies according to the incident angle at which they intersect the atmosphere. Considering a relatively small incident angle to the atmosphere of 30°, the refraction displacement was found to be less than 0.001 mile. The resolution (defined here as the distance between the points on the earth's surface which correspond to adjacent data points in the image) in the radial direction for rays having a 30° incident angle was about 1.5 miles. At incident angles of 87°, the refraction displacement increased to 8.5 miles while the resolution grew to greater than 30 miles.

In calculating the refractions it was assumed that the clouds were at the earth's surface, which resulted in conservative values. In addition, the atmosphere was considered to consist of three regions of different indices of refraction. It was assumed that the index existing at the lower edge of each zone was effective for the entire zone. This was also quite conservative. Because of the uncertainty of data near the horizon, it was concluded that the atmospheric distortion could be ignored with considerable safety. Although atmospheric distortion effects were found to be negligible compared with the resolution of present weather satellite photography, they may be significant in future, higher resolution systems.

Additional distortions which affect the fidelity of the tonal reproduction have not been considered for reasons stated earlier in the section on generation of digital data. Discussions of this problem are found in most basic photographic and television texts.

Photographic reproduction of processed image data

After the image has been rectified and placed on a digital output tape, it is ready for reproduction on the modified WILD STK-1 unit. For reproduction the A/D converter is used in a digital to analog (D/A) mode, and instead of using a constant CRT spot intensity, the intensity is modulated according to the analog equivalent of the digital gray shade value. The spot is focused to a 2-mil diameter for reproduction. The cathode-ray tube is unblanked for an exposure of 40 μsec at each spot position.

The photographic medium used consists of 9 × 9 in. glass plates having a commercially available emulsion. The plates are developed by normal procedures.

Analysis of digital processing system

• *Examples of rectified images*

The feasibility of the digital rectification of TIROS Weather Satellite images was successfully demonstrated by processing photographs from three sample orbits of the wide-angle camera data. The sample data were furnished by the Geophysics Research Directorate in the form of 35 mm positive film strips.

Typical results from orbit 638 are presented in Fig. 8 together with examples of the original input data (Fig. 6) and pictures which have been scanned and reproduced without digital processing (Fig. 7). A significant feature of the technique is that digital processing does not degrade the data in any way. Noise, geometrical distortion, or loss of data is not introduced by the process unless degradation is purposely introduced by the program. However, a comparison of the original images and images which were scanned and reproduced without digital processing does reveal the effects of the 406-line-per-inch resolution and eight shades of gray used for the feasibility demonstration.

With the digitized image in Fig. 7 serving as input data, the sample frames were processed on an IBM 704. The results were reproduced on the modified WILD equipment using glass plates. The images on the glass plates were positives. Contact negatives of the glass plates were made and paper positive enlargements produced from them.

Orbit 638 covered the eastern section of Africa in the vicinity of the Gulf of Aden and northeast across Saudi Arabia into the Himalayas. Frame 11 shows snow cover on the Himalayas while frames 18 and 19 show relatively clear skies over the Gulf of Oman. Very good landmarks were visible in these two frames. The landmarks were used to check the Mercator projection process by generating a Mercator map of the area from U.S. Air Force maps and overlaying the map on the processed image, shown in Fig. 9. Because the scanning equipment was undergoing constant refinement, the original data was scanned at 406 lines per inch while the reproduction was generated at 470 lines per inch. As a result, the reproduced image is in error by approximately 15 percent in the scanning (horizontal) direction. Measurement of the amount of misfit between the Mercator map and the processed image shows just this amount of east-west error. The horizontal banding evident on the lower right edge of frame 19 is due to the routine which fills in those areas not covered by the skeleton, generated when the area is expanding. The fill-in routine operates by searching for data positions in the output memory section which

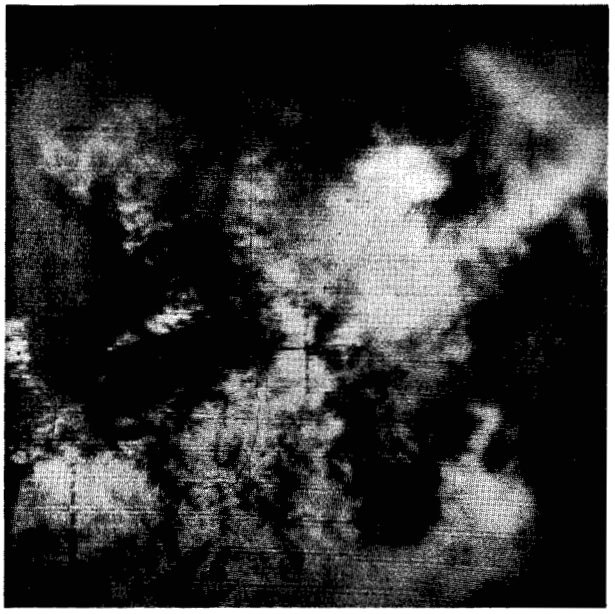

FRAME 11

FRAME 18

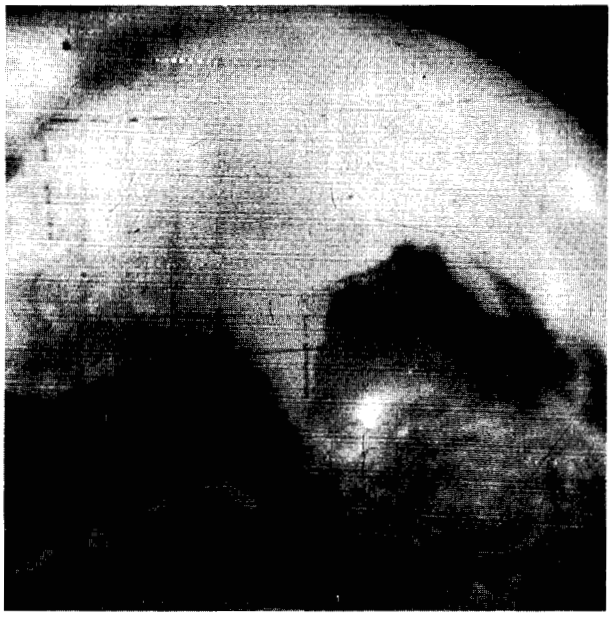

FRAME 19

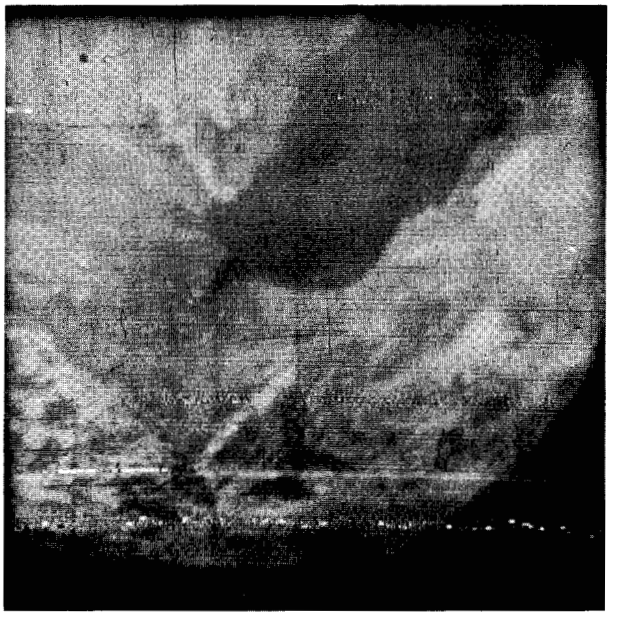

FRAME 29

Figure 6 **Original photographs from orbit 638.**
Reproduced from 35 mm film strips.

have not received any data. This is noted by the absence of a count in the bookkeeping portion of each data character. It places the adjacent shade value into these empty positions.

Because the Mercator image does not fill the output image at low nadir angles, the fill routine, which proceeds from left to right, considers the empty positions to the right of the image data in the same fashion as empty positions in the image proper. The result is that the last shade on the right edge of the image data is "filled in" across the remaining empty positions in that row. This could be readily corrected by introducing a border of black or zero positions around the original image data before it is processed.

Accuracy of results

The Mercator overlay, shown in Fig. 9, represents a good check on the results of the digital processing

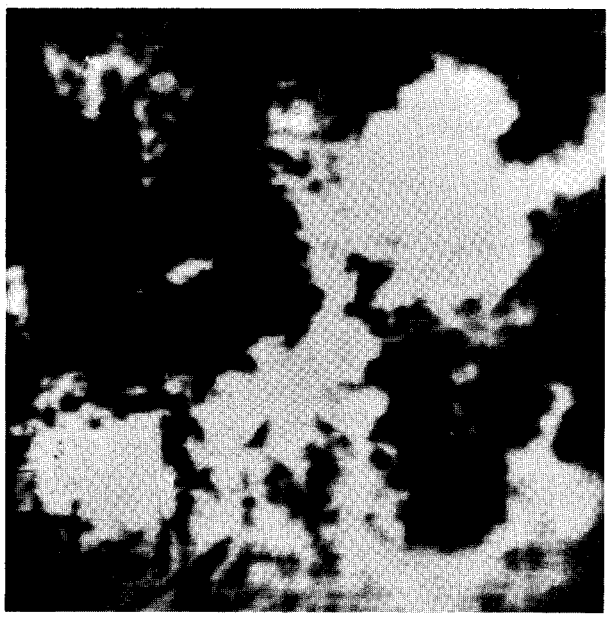

FRAME 11

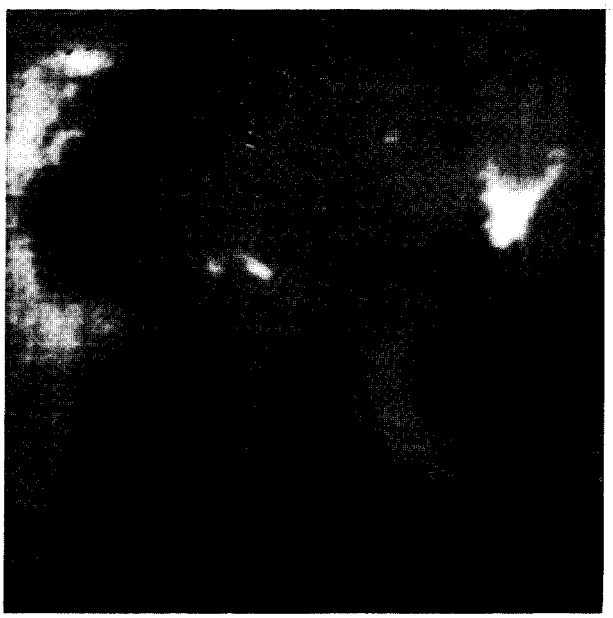

FRAME 18

FRAME 19

FRAME 29

Figure 7 **Scanned and reproduced samples from orbit 638.**

technique. Excepting the 15 percent horizontal error discussed earlier, the fit appears to be quite good. Using the picture-center coordinates which are printed by the IMB 704 as each frame is processed, frame 19 was located on a Mercator grid, and the transparent overlay map was shifted on the image to obtain the best fit of land mass outlines. The resulting mismatch of grids showed that the computer picture center was in error by 1.5° longitude and 0.5° latitude.

Prior to processing the sample frames, an error analysis was performed on the mathematics involved in the processing, which is developed in Appendix 2. The input data errors in Table 1 were used to obtain a predicted rms error in the absolute value of the processed image coordinates.

The predicted rms errors amounted to $\pm 2°$ in longitude and $\pm 4.8°$ in latitude. Taking a particular point in frame 19 as an example, its map coordinates

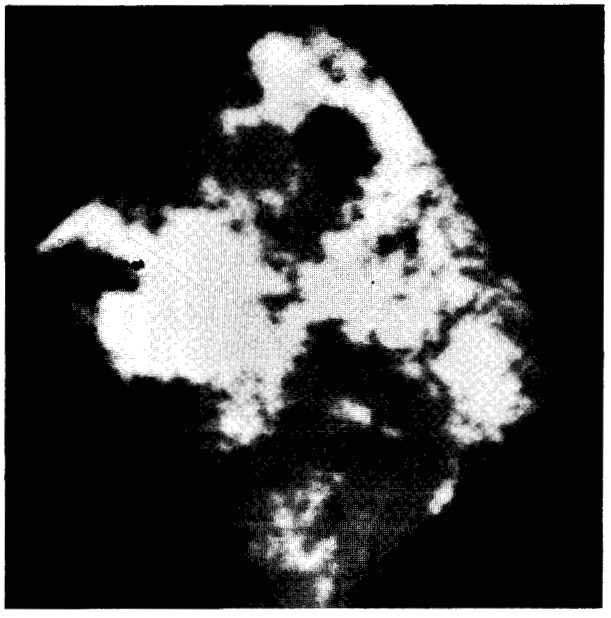

FRAME 11

FRAME 18

FRAME 19

FRAME 29

Figure 8 **Rectified samples from orbit 638.**

were located at 51.59° E, 24.69° N. Using the known input parameters of the selected frame, its coordinates were calculated to be 53.6° E, 21.8° N. This amounted to an error of 2.1° in longitude and 2.8° in latitude. Considering that the coordinates of the reference points were all assumed to be in error by 1° initially, the results are quite satisfactory. The low-error figures obtained from the overlay probably result from the least-squares fit observations which were made visually in matching the map to the image.

Processing time

The time required to manipulate the digital data, including the input and output operations, averages 12 minutes on an IBM 704. This figure could be reduced by an order of magnitude or more by using faster computers and different programming techniques. For example, processing the program, essen-

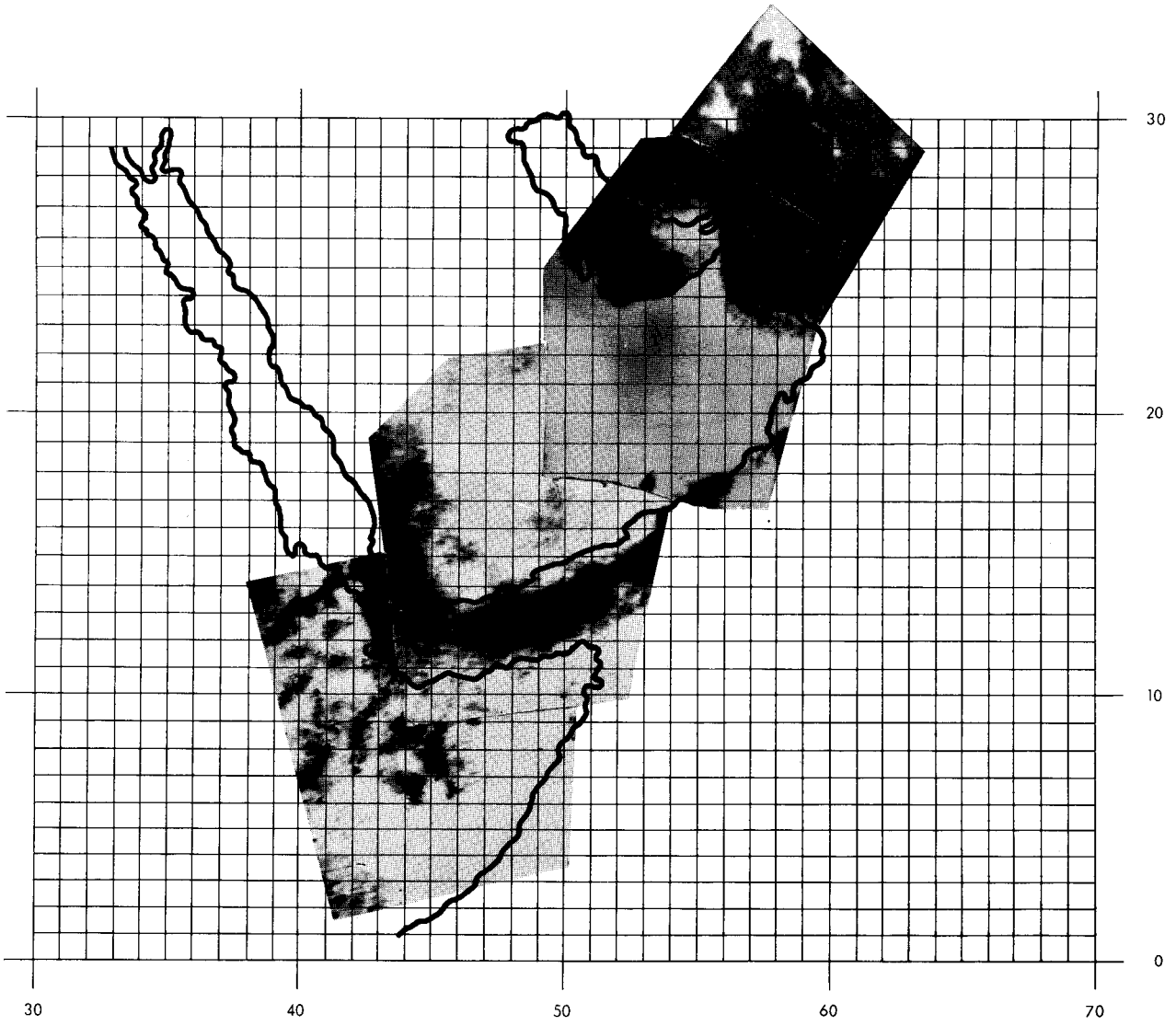

Figure 9 **Mercator grid overlay from orbit 638.**
Includes frames 16, 19, 23 and 27.

tially unchanged on a solid-state IBM 7090 would reduce the processing time by a factor of about 5.

An original data field of 300 × 300 characters representing the 0.75 × 0.75 inch image constitutes 90,000 input data characters. The complete transformation of the image to Mercator map coordinates is performed on approximately 22,000 to 32,000 data points, depending on the amount of detail in the image. Comparing these figures with the input of 90,000 characters shows that the condensation factor obtained by redundancy reduction is between 2.8 and 4.1.

If a new program were to be generated based on the knowledge gained in this project, the present detail-dependent method of reducing redundancy would probably be waived in favor of a scheme based on selecting points for mapping on a position basis. We have found that at least six points can always be traversed in TIROS photographic data before excessive

Table 1 **Input data errors.**

Latitude and longitude of principal points	±1°
Latitude and longitude of sub-satellite points	±1°
Altitude of satellite	0.2×10^6 cm
Nadir angle	±1°
Image orientation angle	±1.5°

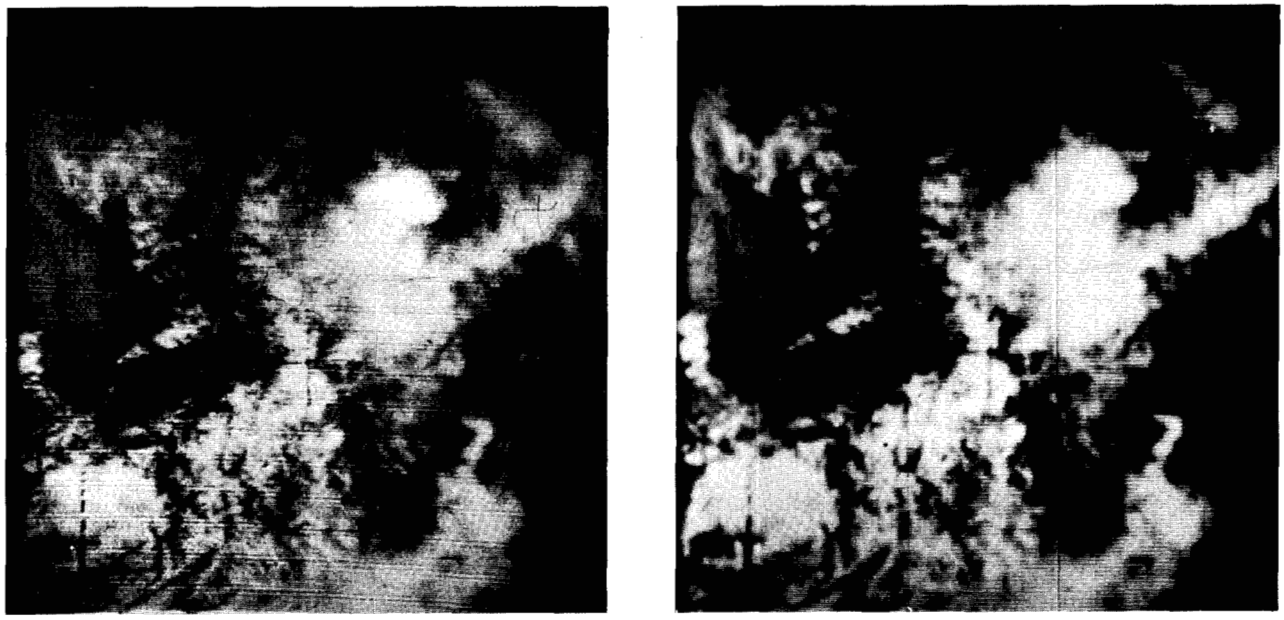

Figure 10 **Comparison of original image (left) with digitized image (right) using 500 line resolution and 32 transmissivity steps.**

curvature of the output ensues (using 400 lines per inch resolution). Thus a point selection scheme based on grid position and using linear interpolation to fill the intermediate areas looks most promising.

Summary

During the Weather Satellite Photo Rectification study, sample photographs from TIROS I have been digitized and successfully rectified using a digital computer. Using approximately 400 lines per inch resolution and a fixed-output format, the data can be processed in about 12 minutes on an IBM 704 computer, depending on the detail present in the picture.*

Obtaining a Mercator projection of an area of the earth's surface by digital manipulation leads to the conclusion that other types of outputs can be obtained by manipulating the data in different ways. Outputs using various map projection systems could be developed using appropriate mathematics. In addition, outlines of areas could be superimposed by mapping shade change points only.

Increasing the speed of processing could be achieved through the use of revised programming techniques, some of which have already become apparent after the first attempt at digital rectification of satellite photography. In addition, the obvious step of using higher-speed, solid-state data processing equipment is available.

Means of including grid coordinate lines on the output image have been developed, see front cover. The final phase of work will investigate methods of automatically forming a mosaic of adjacent pictures from a single orbit.

Appendix 1: Matrix transformation rectification

The origin of No. 6 coordinate system is taken to be the perspective point of the photograph. The principal axis passes through this point and is taken as the z_6 axis. The plane of the photo is perpendicular to this axis and a distance f from the origin in the negative direction. The direction of the x_6 axis is taken parallel to a scan line in the photograph. The No. 6 coordinate system must be rotated about the z_6 axis to a No. 5 coordinate system which has its x_5 axis coincident with the principal line in the photograph, as illustrated in Fig. 11.

The following matrix equation gives the coordinates relative to the No. 5 system in terms of the coordinates of the original No. 6 system:

$$\xi_5 = R_{z_6}\xi_6$$

$$\begin{bmatrix} x_5 \\ y_5 \\ z_5 \end{bmatrix} = \begin{bmatrix} \cos\gamma & +\sin\gamma & 0 \\ -\sin\gamma & \cos\gamma & 0 \\ 0 & 0 & 1 \end{bmatrix} \begin{bmatrix} x_6 \\ y_6 \\ z_6 \end{bmatrix}.$$

A rotation about the y_5 axis through the nadir angle τ brings the No. 5 system to the No. 4 system. This rotation, shown in Fig. 12, has its z_4 axis coincident with the nadir axis and its x_4 axis lies in the principal plane of the photo. The following transformation describes this rotation:

$$\xi_4 = R_{y_5}\xi_5$$

* *Note added in proof:* Figure 10 shows a sample produced with 500 lines resolution and 32 transmissivity levels, demonstrating the quality obtainable with digital techniques.

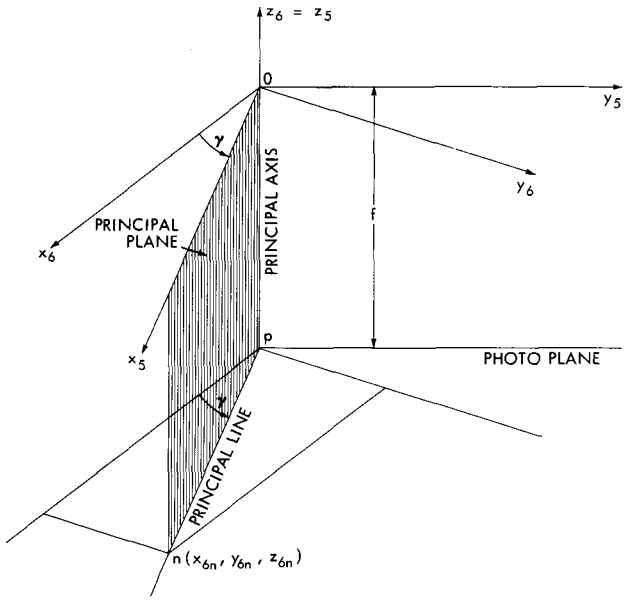

Figure 11 **Local coordinates.**
$z_{6_n} = -f$; $\theta_{6_n} = \arctan(y_{6_n}/x_{6_n})$; $\gamma = -\theta_{6_n}$.

$$\begin{bmatrix} x_4 \\ y_4 \\ z_4 \end{bmatrix} = \begin{bmatrix} +\cos\tau & 0 & +\sin\tau \\ 0 & 1 & 0 \\ -\sin\tau & 0 & +\cos\tau \end{bmatrix} \begin{bmatrix} x_5 \\ y_5 \\ z_5 \end{bmatrix} .$$

Combining the two rotations, the transformation from the No. 6 to the No. 4 system is obtained:

$$\xi_5 = R_{z_6}\xi_6 , \qquad \xi_4 = R_{y_4}\xi_5$$

$$\xi_4 = R_{y_4}(R_{z_6}\xi_6)$$

$$\xi_4 = (R_{y_4}R_{z_6})\xi_6 = R_{64}\xi_6$$

$$R_{64} = \begin{bmatrix} +\cos\tau\cdot\cos\gamma & +\cos\tau\cdot\sin\gamma & +\sin\tau \\ -\sin\gamma & +\cos\gamma & 0 \\ -\sin\tau\cdot\cos\gamma & -\sin\tau\cdot\sin\gamma & +\cos\tau \end{bmatrix} .$$

The coordinates of a point on the surface of a sphere representing the earth can also be described in the No. 4 coordinate system.

If the coordinates of a point, a, in the picture are x_{4_a}, y_{4_a}, z_{4_a}, the equations for the line through the origin of the coordinate system and the point in the picture are

$$x_4/x_{4_a} = y_4/y_{4_a} ,$$

$$y_4/y_{4_a} = z_4/z_{4_a} .$$

If the length of the vector from the origin to the center of the earth is ρ, and the radius of the earth is R, the equation for the sphere approximating the earth in the No. 4 coordinate system is

$$x_4^2 + y_4^2 + (z_4 + \rho_r)^2 = R^2 .$$

Solving these three equations in terms of z_4

$$x_4 = z_4(x_{4_a}/z_{4_a}) , \qquad y_4 = z_4(y_{4_a}/z_{4_a})$$

$$z_4^2(x_{4_a}/z_{4_a})^2 + z_4^2(y_{4_a}/z_{4_a})^2 + (z_4 + \rho)^2 - R^2 = 0$$

$$[1 + (x_{4_a}/z_{4_a})^2 + (y_{4_a}/z_{4_a})^2]z_4^2 + 2\rho z_4 + (\rho^2 - R^2) = 0$$

$$z_4 = (-\rho + \sqrt{\rho^2 - A(\rho^2 - R^2)})/A ,$$

where

$$A = 1 + (x_{4_a}/z_{4_a})^2 + (y_{4_a}/z_{4_a})^2 .$$

By a single translation of the No. 4 system along the z_4 axis through the distance ρ, the No. 3 system is obtained.

x_3, y_3, z_3 represent the coordinates of the image point, a, on the surface of the sphere. The origin of the No. 3 system is at the center of the sphere. The polar axis of this sphere is coincident with the nadir axis of the photo image plane. To obtain the true earth coordinates of the point, three additional rotations of the No. 4 system are required.

The first rotation is about the z_3 axis through the angle θ_{2_p}. This rotation generates the No. 2 coordinate system. θ_{2_p} is the longitude of the principal point as expressed in the No. 2 system.

$$\theta_{2_p} = \tan^{-1}(y_{2_p}/x_{2_p}) .$$

x_{2_p} and y_{2_p} are obtained from application of the

Figure 12 **Rotation through nadir angle.**
0 = perspective point of photograph; n = sub-satellite point; p = image principal point; τ = nadir angle.

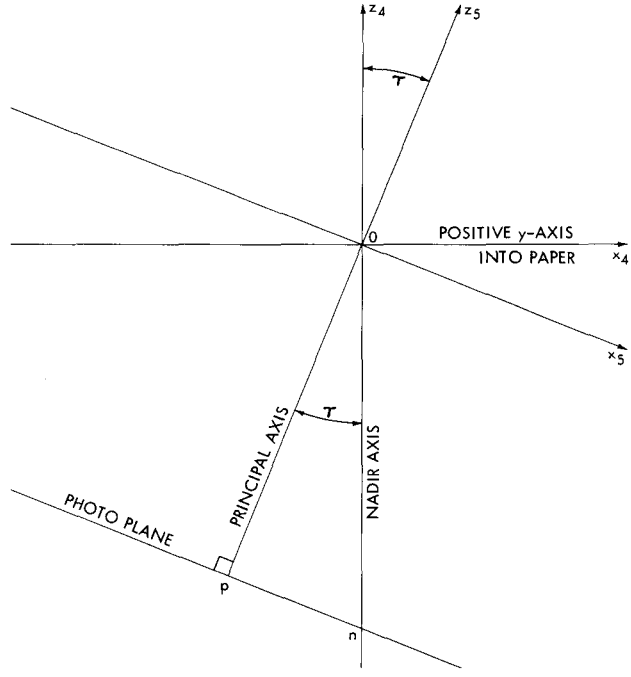

matrix R_{02} (developed below) to ξ_{0_p}.

The second rotation is taken about the y_2 axis through angle $\bar{\phi}_{0_n}$. This angle represents the colatitude of the nadir points as described in true earth coordinates.

The final rotation is about the z_1 axis through angle θ_{0_n}. This angle is the longitude of the true earth nadir point. This final rotation yields the 0 coordinate system which represents true earth coordinates. The three rotations may be combined as follows:

$$\xi_0 = R_{02}R_{z_3}\xi_3 ,$$

where

$$R_{02} = \begin{bmatrix} \cos\bar{\phi}_{0_n}\cos\theta_{0_n} & -\sin\theta_{0_n} & \sin\bar{\phi}_{0_n}\cos\theta_{0_n} \\ \cos\bar{\phi}_{0_n}\sin\theta_{0_n} & \cos\theta_{0_n} & \sin\bar{\phi}_{0_n}\sin\theta_{0_n} \\ -\sin\bar{\phi}_{0_n} & 0 & \cos\bar{\phi}_{0_n} \end{bmatrix}$$

and

$$R_{z_3} = \begin{bmatrix} -\cos\theta_{2_p} & -\sin\theta_{2_p} & 0 \\ \sin\theta_{2_p} & -\cos\theta_{2_p} & 0 \\ 0 & 0 & 1 \end{bmatrix} .$$

Using x_0, y_0, z_0, the latitude and longitude of the point may be described. In addition, the corresponding Mercator map coordinates can be defined as follows:

$$y_m = (R_1/2)\ln\left[\frac{1+(z_0/R)}{1-(z_0/R)}\right]$$

$$x_m = R_1 \tan^{-1}(y_0/x_0) .$$

R_1 is the radius of the model earth used to generate the scaled Mercator projection.

Appendix 2: Error analysis—matrix rectification

$$\xi_4 = R_{64}\xi_6$$

$$dx_{4_a} = \{[(\cos\tau\cos\gamma)dx_6]^2 + [(\cos\tau\sin\gamma)dy_6]^2 + [(+\sin\tau)df]^2 + [(-x_6\cos\gamma\sin\tau - y_6\sin\tau\sin\gamma + f\cos\tau)d\tau]^2 + [(-x_6\cos\tau\sin\gamma + y_6\cos\tau\cos\gamma)d\gamma]^2\}^{1/2}$$

$$dy_{4_a} = \{[(\sin\tau\sin\gamma)dx_6]^2 + [(\cos\gamma)dy_6]^2 + [(x_6\sin\gamma\cos\tau)d\tau]^2 + [(x_6\sin\tau\cos\gamma - y_6\sin\gamma)d\gamma]^2\}^{1/2}$$

$$dz_{4_a} = \{[(+\sin\tau\cos\gamma)dx_6]^2 + [(+\sin\tau\sin\gamma)dy_6]^2 + [(+\cos\tau)df]^2 + [(-x_6\cos\gamma\cos\tau - y_6\sin\gamma\cos\tau - f\sin\tau)d\tau]^2 + [(x_6\sin\tau\sin\gamma - y_6\sin\tau\cos\gamma)d\gamma]^2\}^{1/2} .$$

Let $\beta = [\rho^2 - A(\rho^2 - R^2)]^{1/2}$

$$\partial z_4/\partial\rho = (-\rho/A) + (1/A)[\rho^2 - A(\rho^2 - R^2)]^{-1/2} \times [\rho(1-A)]$$

$$\partial z_4/\partial x_{4_a} = (1/{z_{4_a}}^2)\{(2\rho/A^2)x_{4_a} - [(2x_{4_a}/A^2)\beta + (x_{4_a}/A\beta)]\}$$

$$\partial z_4/\partial y_{4_a} = (1/{z_{4_a}}^2)\{(2\rho/A^2)y_{4_a} - [(2y_{4_a}/A^2)\beta + (y_{4_a}/A\beta)]\}$$

$$\partial z_4/\partial z_{4_a} = (1/2A{z_{4_a}}^3)[(2\beta/A) + (1/\beta) - (2\rho/A)] \times ({x_{4_a}}^2 + y_{4_a})$$

$$dz_4 = \{[(\partial z_4/\partial x_{4_a})dx_{4_a}]^2 + [(\partial z_4/\partial y_{4_a})dy_{4_a}]^2 + [(\partial z_4/\partial z_{4_a})dz_{4_a}]^2 + [(\partial z_4/\partial\rho)d\rho]^2\}^{1/2}$$

$$\partial x_4/\partial x_{4_a} = z_4/z_{4_a}$$

$$\partial x_4/\partial z_{4_a} = -x_{4_a}z_4/{z_{4_a}}^2$$

$$\partial x_4/\partial z_4 = x_{4_a}/z_{4_a}$$

$$dx_4 = \{[(\partial x_4/\partial x_{4_a})dx_{4_a}]^2 + [(\partial x_4/\partial z_{4_a})dz_{4_a}]^2 + [(\partial x_4/\partial z_4)dz_4]^2\}^{1/2} .$$

Similarly for dy_4

$$dy_4 = \{[(\partial y_4/\partial z_4)dz_{4_a}]^2 + [(\partial y_4/\partial y_{4_a})dy_{4_a}]^2 + [(\partial y_4/\partial z_{4_a})dz_{4_a}]^2\}^{1/2}$$

$$x_3 = x_4 , \quad y_3 = y_4 \quad \text{and} \quad z_3 = \rho + z_4 .$$

Therefore,

$$dx_3 = dx_4 , \quad dy_3 = dy_4 , \quad dz_3 = dz_4 .$$

Assuming the following typical values for input parameters and their errors:

$dx_i = dy_i = 2 \times 10^{-3}$ cm	$h = 73.4 \times 10^6$ cm
$d\gamma = 1.5°$	$R = 637.12 \times 10^6$ cm
$d\gamma = 1°$	$\rho = 710.52 \times 10^6$ cm
$d\rho = 0.2 \times 10^6$ cm	$f = 1.44$ cm.

We obtain the following:

$dx_3 = 1.73 \times 10^6$ cm	$x_3 = 62.40 \times 10^6$ cm
$dy_3 = 0.77 \times 10^6$	$x_3 = 17.85 \times 10^6$
$dz_3 = 1.40 \times 10^6$	$z_3 = 633.90 \times 10^6$.

Errors encountered in transferring the x_3, y_3, z_3 coordinates to the Mercator projection are treated next.

Applying the transformation $\xi_0 = R_{02}\cdot R_{z_3}\cdot\xi_3$ (Appendix 1) to the No. 3 coordinates, we obtain

$$x_0 = 351.04 \times 10^6 \text{ cm}$$

$$y_0 = 476.19 \times 10^6$$

$$z_0 = 236.51 \times 10^6 .$$

To determine the errors in the calculation of the true earth coordinate system, dx_0, dy_0, dz_0 requires consideration of the errors present in the geographical coordinates of the principal point and sub-points of the photographic image. If we know $d\theta_{0_p}$, $d\phi_{0_p}$ and $d\theta_{0_n}$, $d\bar{\phi}_{0_n}$ we can find

$$dx_{0_p} = -R \sin \theta_{0_p} d\theta_{0_p}$$

$$dy_{0_p} = R \cos \theta_{0_p} d\theta_{0_p}$$

$$dz_{0_p} = -R \cos \phi_{0_p} d\phi_{0_p} .$$

To determine the error in the angle θ_{2_p} which appears in R_{z_3} requires calculation of dx_{2_p}, dy_{2_p}.

$$\begin{aligned} dx_{2_p} = \{&(\cos \bar{\phi}_{0_n} \cos \theta_{0_n} dx_{0_p})^2 + [(x_{0_p} \cos \theta_{0_n} \sin \bar{\phi}_{0_n} \\ &+ y_{0_p} \sin \theta_{0_n} \sin \bar{\phi}_{0_n} - z_{0_p} \cos \bar{\phi}_{0_n}) d\bar{\phi}_{0_n}]^2 \\ &+ (\cos \bar{\phi}_{0_n} \sin \theta_{0_n} dy_{0_p})^2 \\ &+ [(-x_{0_p} \cos \bar{\phi}_{0_n} \sin \theta_{0_n} \\ &+ y_{0_p} \cos \bar{\phi}_{0_n} \cos \theta_{0_n}) d\theta_{0_n}]^2 \\ &+ (\sin \bar{\phi}_{0_n} dz_{0_p})^2 \}^{1/2} \end{aligned}$$

$$\begin{aligned} dy_{2_p} = \{&(\sin \theta_{0_n} dx_{0_p})^2 + (\cos \theta_{0_n} dy_{0_p})^2 \\ &+ [(x_{0_p} \cos \theta_{0_n} + y_{0_p} \sin \theta_{0_n}) d\theta_{0_n}]^2 \}^{1/2} . \end{aligned}$$

Then

$$\begin{aligned} d\theta_{2_p} = &\frac{1}{1 + (y_{2_p}/x_{2_p})^2} \\ &\times \{[(y_{2_p}/x_{2_p}{}^2) dx_{2_p}]^2 + [(1/x_{2_p}) dy_{2_p}]^2 \}^{1/2} \end{aligned}$$

$$\begin{aligned} dx_0 = \{&[(-x_3 \cos \theta_{0_n} \cos \theta_{2_p} \sin \bar{\phi}_{0_n} - y_3 \cos \theta_{0_n} \\ &\times \sin \theta_{2_p} \sin \bar{\phi}_{0_n} + z_3 \cos \theta_{0_n} \cos \bar{\phi}_{0_n}) d\bar{\phi}_{0_n}]^2 \\ &+ [(-x_3 \sin \theta_{0_n} \cos \theta_{2_p} \cos \bar{\phi}_{0_n} + x_3 \cos \theta_{0_n} \\ &\times \sin \theta_{2_p} - y_3 \sin \theta_{0_n} \sin \theta_{2_p} \cos \bar{\phi}_{0_n} \\ &- y_3 \cos \theta_{0_n} \cos \theta_{2_p} - z_3 \sin \theta_{0_n} \sin \bar{\phi}_{0_n}) d\theta_{0_n}]^2 \\ &+ [(-x_3 \cos \theta_{0_n} \sin \theta_{2_p} \cos \bar{\phi}_{0_n} + x_3 \sin \theta_{0_n} \\ &\times \cos \theta_{2_p} + y_3 \cos \theta_{0_n} \cos \theta_{2_p} \cos \bar{\phi}_{0_n} \\ &+ y_3 \sin \theta_{0_n} \sin \theta_{2_p}) d\theta_{2_p}]^2 \\ &+ [(\cos \theta_{0_n} \cos \theta_{2_p} \cos \bar{\phi}_{0_n} \\ &+ \sin \theta_{0_n} \sin \theta_{2_p}) dx_3]^2 \\ &+ [(\cos \theta_{0_n} \sin \theta_{2_p} \cos \bar{\phi}_{0_n} \\ &- \sin \theta_{0_n} \cos \theta_{2_p}) dy_3]^2 \\ &+ [(\cos \theta_{0_n} \sin \bar{\phi}_{0_n}) dz_3]^2 \}^{1/2} . \end{aligned}$$

Similar expressions can be obtained for dy_0 and dz_0. Using the error values obtained for x_3, y_3, z_3 and assuming errors in the input latitude and longitude values of 1°,

$$dx_0 = 13.30 \times 10^6 \text{ cm}$$

$$dy_0 = 15.64 \times 10^6$$

$$dz_0 = 16.52 \times 10^6 .$$

Considering the Mercator projection of the general points x_0, y_0, z_0, and taking $R_1 = R$

$$x_m = R_1 \tan^{-1}(y_0/x_0) = 596.02 \times 10^6 \text{ cm}$$

$$y_m = (R_1/2) \ln[(R + z_0)/(R - z_0)] = 248.48 \times 10^6 \text{ cm}$$

$$\begin{aligned} dx_m &= [R_1/(x_0{}^2 + y_0{}^2)](x_0 dy_0 + y_0 dx_0) \\ &= 21.53 \times 10^6 \text{ cm} \end{aligned}$$

$$dy_m = [R_1 R/(R^2 - z_0{}^2)] dz_0 = 19.16 \times 10^6 \text{ cm} .$$

Converting the coordinates to latitude and longitude, we obtain

$$\theta = 53.6° \qquad d\theta = 2.0°$$

$$\phi = 21.8° \qquad d\phi = 4.8° .$$

The data used in these calculations represent an actual point taken from frame 19 of orbit 638. From the map used to determine the principal and sub-point coordinates, this point is located at

$$\theta = 51.5°$$

$$\phi = 24.6° .$$

Thus the actual errors are:

$$\theta \text{ error} = 2.1°$$

$$\phi \text{ error} = 2.8° .$$

These values compare well with the calculated rms errors.

Acknowledgments

The authors would like to express their thanks to M. E. Boyd and F. A. Fogg who made contributions to the mathematical analysis, and to L. L. Ackerman, J. A. Dickerson and J. R. Ralston who provided the digitized photographic data.

References

1. W. K. Widger, "Contributions to Satellite Meteorology," *GRD Research Notes*, No. 36, Geophysics Research Directorate, Air Force Cambridge Research Center, Bedford, Mass., 1960.
2. F. R. Valovcin, "Contributions to Satellite Meteorology," *GRD Research Notes*, **2**, No. 36, Geophysics Research Directorate, Air Force Cambridge Research Center, Bedford, Mass., 1961.
3. A. H. Glaser, "Meteorological Utilization of Images of the Earth's Surface Transmitted from a Satellite Vehicle," Contract AF 19 (604) 1589, Phase II, Geophysics Research Directorate, Air Force Cambridge Research Center, Bedford, Mass., 1957.

4. A. H. Glaser, "TIROS Meteorology," Final Report, Contract AF 19 (604) 1589, Geophysics Research Directorate, Air Force Cambridge Research Center, Bedford, Mass., 1961.
5. W. K. Widger, "Examples of Project TIROS Data and Their Practical Meteorological Use," *GRD Research Notes*, No. 38, Geophysics Research Directorate, Air Force Cambridge Research Center, Bedford, Mass., 1960.
6. E. A. Goldberg and V. D. Landon, "Key Equipment for TIROS I," *Astronautics*, **5**, 36 (June 1960).
7. J. E. Keigler and C. B. Oakley, "The TIROS System on the Ground," *Astronautics*, **5**, 44 (June 1960).

Received March 14, 1962